

Zero-bias Rectifying performance Enhancement of MIM Tunneling Diodes by Geometric Field Enhancement and Boiling Water Oxidation

Kwangsik Choi, Filiz Yesilkoy, Geunmin Ryu, Mario Dagenais, and Martin Peckerar

Department of Electrical and Computer Engineering, University of Maryland, College Park, Maryland 20740

Metal-Insulator-Metal (MIM) tunneling diodes have potential application as rectifying, mixing, and harmonic generating devices operating at infrared frequencies. Our research focuses on the rectifying performance of MIM diodes for infrared energy harvesting application. The rectified DC current and voltage are proportional to the second derivative (I'') of tunneling current and the sensitivity factor (S) of a given MIM tunneling diode. Here, the sensitivity is defined as I''/I' where the I' is the first derivative of tunneling current. Generally, the rectifying performance of current thin-film MIM tunneling diodes is not sufficient to be used for energy harvesting due to low sensitivity factors. Also, the diode needs to be operated at some DC bias point to get the highest S for the maximum rectifying output. This basic condition leads to excess dissipation. That is, the power consumption exploited for biasing a given tunneling diode may be higher than the rectified and harvested power. Zero-bias operation is therefore most desirable for energy harvesting applications.

In this paper we describe how improved the rectifying performance at zero-bias by using a geometric field enhancement (GFE) technique. This technique has been proposed and demonstrated in Poly-Si/SiO₂/Ti-Au and Ni/NiO/Ni tunneling diodes^{1, 2}. Using the technique, unique asymmetric tunneling diodes have been implemented successfully. Figure 1 shows the fabricated MIM tunneling diodes using a Ni/NiO/Ni structure. The Type-A structure shown is an asymmetric tunneling diode implemented to exploit the GFE technique, and the Type-B diode is a simple overlap tunneling diode prepared as a reference. The diodes are processed using e-beam patterning and a metal lift-off process, and the oxidation is performed using an oxygen plasma process for a tunneling barrier (NiO) with time used as an experimental variable. The measured DC asymmetric tunneling current and the I'' for a Type-A diode are shown in Figure 2. In contrast, Type-B diodes show almost symmetric a current-voltage relationship. RF rectification tests have been performed to check rectifying performance of fabricated diodes. We used 6.4 GHz RF signal with 12 dBm RF power to show the rectifying performance of these structures. Figure 3 shows the rectified DC current of the diodes used in Figure 2.

Each diode's zero-bias rectifying performance is listed at Table 1. For proper comparison, diodes are selected to have similar tunneling current level or resistance and sorted into each group. In group I, the two diodes have comparable tunneling resistance and junction size, but the I'' and S of Type-A diode is about nine times higher than Type-B diode. For the higher I'' , much higher DC rectified current is obtained from the Type-A diode in group I. For group II and III, a similar result is observed. This result demonstrates that the GFE technique improves the rectifying performance at zero-bias, especially by providing higher I'' .

For further improvement at zero-bias, we focused on decreasing the diode's forward resistance to achieve higher I'' . As mentioned above, the tunneling barrier of the diodes in group I ~ III are obtained using an oxygen plasma treatment, and the tunneling resistances are higher than that obtained in the other processes discussed. Applying the boiling oxidation process¹ to the Ni surface of the first electrode, we achieve very low tunneling resistances. Figure 4 shows the measured DC current-voltage data for a Ni/NiO/Ni tunneling diode which has a tunneling barrier implemented by boiling water oxidation process. In Table 1, the last two diodes show superior DC rectified currents due to the increased I'' . In these low tunneling resistance diodes, we achieved as much as three orders of magnitude higher I'' .

¹Kwangsik Choi, Mario Dagenais, and Martin Peckerar, "Fabrication of Thin Film Asymmetric Tunneling Diode using Geometric Field Enhancement," in *Semiconductor Device Research Symposium, 2009. ISDRS '09. International*, 2009, pp. 1-2.

²Kwangsik Choi, Geunmin Ryu, Filiz Yesilkoy, Athanasios Chryssis, Neil Goldsman, Mario Dagenais, and Martin Peckerar, "Geometry Enhanced Asymmetric Rectifying Tunneling Diodes," *Journal of Vacuum Science and Technology B* 28, C6O50, 2010.

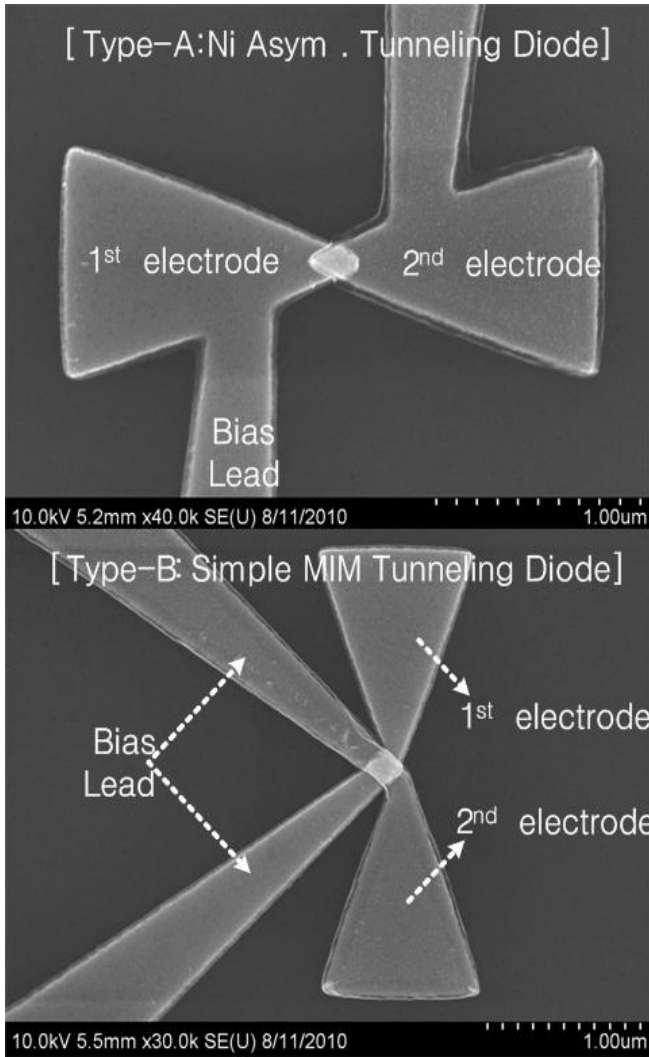


Figure 1. SEM images of completed MIM tunneling diodes using Ni/NiO/Ni structure. Type-A is an asymmetric tunneling diode implemented by using GFE technique, and Type-B diode is a simple overlap tunneling diode prepared for a reference to compare performance.

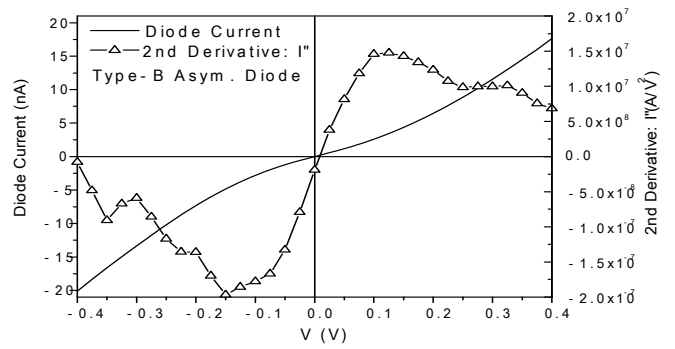


Figure 2. Measured DC current-voltage data (solid line) and extracted nonlinearity (I'') (triangle line) for a Type-A asymmetric tunneling diode with $0.013 \mu\text{m}^2$ junction area.

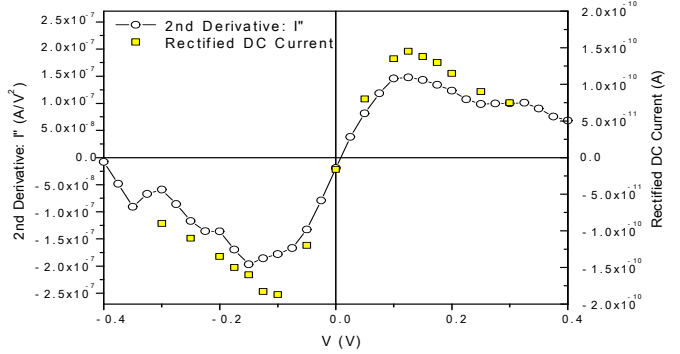


Figure 3. RF rectifying result of the diode in Figure 2. RF rectifying is performed using transmission antenna and a RF source with 12 dBm at 6.4GHz.

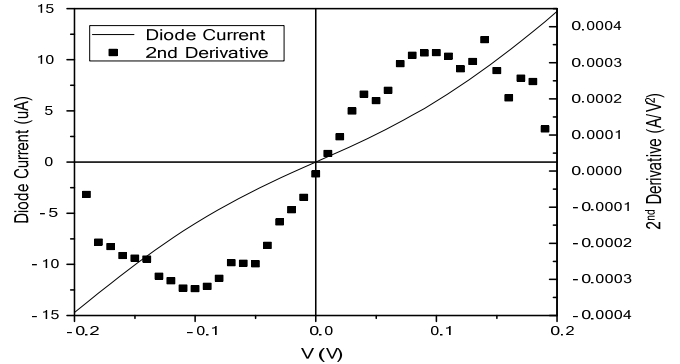


Figure 4. Measured DC current-voltage data (solid line) and extracted nonlinearity (I'' : square) of a Type-A tunneling diode processed by boiling water oxidation ($0.013 \mu\text{m}^2$ junction area).

Table 1. Zero-bias parameters and rectifying results.

Group #	Diode TYPE	Junction AREA [μm^2]	Zero-bias Result				
			Tunneling Current [A]	Differential Resistance [Ω]	Nonlinearity I'' [A/V^2]	Sensitivity S [$1/\text{V}$]	Rectified DC Current [A]
I	A	0.037	-7.0E-12	13.6M	-8.27E-8	-1.12	-4.7E-11
	B	0.029	-4.21E-12	15.3M	-0.91E-8	-0.14	-2.0E-12
II	A	0.018	-2.03E-12	42.4M	-1.91E-8	-0.81	-1.65E-11
	B	0.012	2.05E-12	23.4M	1.32E-8	0.31	1.15E-11
III	A	0.024	-2.1E-13	342M	-1.39E-9	-0.48	-1.35E-12
	B	0.030	-2.1E-13	181M	-0.82E-9	-0.15	-8.0E-13
Boiling water oxidation	A	0.013	-2.4E-9	19K	-8.28E-6	-0.16	-9.0E-9
		0.003	-5.0E-10	150K	-4.7E-7	-0.07	-15.0E-9